

State of Charge Estimation Using Extended Kalman Filters for Battery Management System

Carlo Taborelli, Simona Onori, *Member, IEEE*

Abstract—In this work, the problem of battery state of charge estimation is investigated, using a model based approach. An experimentally validated model of a battery pack produced by AllCell Technologies¹, specific for light electric vehicle (electric scooter or bicycles) is being used to design two state of charge estimation algorithms. An Extended Kalman Filter (EKF) for the state of charge estimation is developed. An adaptive version (AEKF) is presented, in order to adaptively set a proper value of the model noise covariance using the information coming from the on-line innovation analysis. A comparison between the two approaches is conducted and shows that AEKF can consider the problem of incorrect value of the model noise covariance matrix with a reduction of the estimation error. The main idea is to propose an accurate and not too computational demanding algorithm for small vehicle BMS application.

Index Terms—Estimation; Battery; Kalman filter; Adaptive.

I. INTRODUCTION - MOTIVATION

Light Electric vehicles such as electric bikes or scooters offer many benefits over their traditional counterparts such as range, e-bikes and e-scooters can go further than conventional bicycles with little effort. The e-bikes are easier to pedal! They can be quickly recharged anywhere that you can find a power supply, or low batteries can be swapped instantly with fully charged batteries.

As technology advances, many electric vehicle batteries are now also required to communicate with other components within the vehicle such as the motor controller to maximize range and acceleration. An accurate estimation of the energy available inside the battery is essential to excellent powertrain operation and prevent stranding the rider. Lastly, knowing the remaining energy also helps prevent overcharge and overdischarge of batteries, vital to safe use and long life of lithium-ion batteries.

Lithium-ion batteries have become the battery of choice not only for hybrid and electric car, but also for electric bicycle and scooter applications. The key drivers are their high specific energy, energy density, cycle/calendar life as well as their reduced need for maintenance as compared to flooded lead acid batteries. One of their few drawbacks is the difficulty estimating the amount of remaining energy.

Carlo Taborelli is currently a visiting scholar at Clemson University International Center of Automotive Research, Greenville, SC, 29607, USA. carlo.taborelli@mail.polimi.it

Simona Onori is with Department of Automotive Engineering, Clemson University, Greenville, SC, 29607, USA. Phone: (864) 283-7217 sonori@clemson.edu

¹AllCell Technologies LLC, 2321 W. 41st St. Chicago, IL 60609 USA

Different methods have been developed for estimating battery state of charge (SoC). Following the Coulomb counting definition, SoC is evaluated as the ratio between the current capacity, as the integral of the battery current, and the nominal capacity of the battery [1]. This approach shows the drawbacks related to the integral operation computed on the current measurement: it is very sensitive to the SoC initial condition not always known precisely, and the integration can easily diverge in case of additional noise [2].

For these reasons other methods have been investigated, especially for vehicle on-board application based on real measurement, as the case of e-bikes considered in this paper. Extended Kalman filter (EKF) is a powerful model-based estimator suitable for the purpose of this work.

In indirect methods, SoC is evaluated using information from other estimated quantities. SoC can be computed starting from open circuit voltage (V_{OCV}) measurement [3]. In fact, Lead-Acid and Li-ion batteries V_{OCV} is direct function of SoC and this relationship is usually experimentally evaluated. For Lead-Acid batteries in particular, the SoC estimation is straight-forward due to the linear decrease of the V_{OCV} with reference to SoC . By contrast, Li-ion batteries does not present a linear relationship between V_{OCV} and SoC , so that it is harder to translate the V_{OCV} measurement to SoC [1], [4].

Some similar indirect methods are developed using reduced state space electrochemical models, which give a good description of the process inside the battery, together with EKF, in a form that can be used for online SoC and parameters estimations [5] [6].

Other kind of methods have been used in literature as well artificial neural networks and impedance spectroscopy. These methods usually require a greater computational effort compared with EKF and very accurate measurements [7]; this make them suitable for laboratory application [1].

EKF is a successful model-based method for state estimation, widely used also for battery application. SoC estimation with EKF is performed in [8]–[11].

In this work the problem of SoC estimation with EKF is addressed for a Li-ion battery developed for e-bike application. The main purpose is to design a reliable and sophisticated algorithm as EKF for an accurate detection of SoC for the new categories of light vehicle such as e-bikes.

In Section II the battery pack structure is discussed and the mathematical model is introduced. In Section III model parameters are identified: for the battery resistance a dependence on SoC is defined. The SoC estimation algorithm is presented in Section IV where an adaptive version of EKF

is also explained.

II. BATTERY MODELING

In this section a brief description of the battery pack is provided and a mathematical model of the battery is defined.

A. Battery Pack Topology

The battery pack, designed for an e-bike application, is made by 40 LG ICR18650MG1 cells, with a structure *10s4p*: a series of 10 *modules*, each of 4 cells in parallel. A measurement of the voltage across each module is available, as well as the pack input current, being the same in all 10 modules in series.

In this work an average cell model is considered. The average cell voltage is computed in the Battery Management System (BMS) as the average of the 10 voltage measurements across the 10 modules. The average cell capacity is evaluated considering that each of the 40 LG ICR18650MG1 cell in the pack has a rated capacity value of 2.6 Ah. With reference to the battery pack structure, $Q_{nom} = 10.4 \text{ Ah}$ is the capacity of the average cell, as well as the nominal pack capacity.

B. Battery Cell Model

In order to develop a model-based *SoC* estimator, the battery pack is modeled as an average cell, as discussed in Section II-A. Two categories of models have been proposed to model a lithium-ion batteries: those are electrochemical processes based models [12], or equivalent electric circuit based models [8], [13], [14]. The electrical equivalent circuit based are the ones mostly used for BMS application and system integration [15]. By contrast, electrochemical models usually give a better description of the battery internal chemical processes, but at the same time are computational demanding for BMS use. Starting from electrochemical analysis, an equivalent battery model is defined as an electric equivalent circuit based model in [16], [17]. To achieve this purpose, electrochemical impedance spectroscopy is a technique used to define the model electric impedances [18], [19].

Once the battery model is defined as equivalent electric circuit, the electric parameters identification is not always straightforward, as dependence on *SoC*, temperature or current is introduced. In Section III model parameters are identified and *SoC* dependencies are analyzed.

In the present study, a second order electric circuit based model is considered, as shown in Fig. 1.

The state space formulation in discrete time domain is the following:

$$\begin{cases} SoC(k+1) = SoC(k) - \frac{\Delta t}{Q_{nom}} I(k) \\ V_{CT}(k+1) = e^{-\frac{\Delta t}{\tau_{CT}}} V_{CT}(k) + R_{CT} \left(1 - e^{-\frac{\Delta t}{\tau_{CT}}}\right) I(k) \\ V_{Dif}(k+1) = e^{-\frac{\Delta t}{\tau_{Dif}}} V_{Dif}(k) + R_{Dif} \left(1 - e^{-\frac{\Delta t}{\tau_{Dif}}}\right) I(k) \end{cases} \quad (1)$$

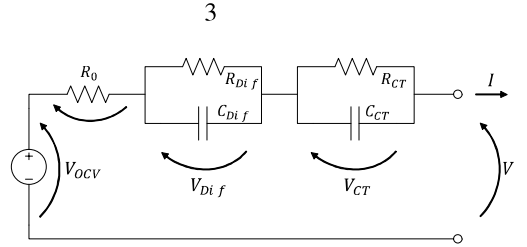


Fig. 1: Equivalent circuit representation of the average cell model

where k is a generic discrete time instant.

The first equation represents the *SoC* dynamic, in which Q_{nom} is the battery nominal capacity and Δt is the discrete time step. The input current $I(k)$ is considered positive during discharging and negative during charging. The two RC parallels (R_{CT}, C_{CT} and R_{Dif}, C_{Dif}) are used to model the dynamic response of the battery cell, and $\tau_{CT} = R_{CT}C_{CT}$ and $\tau_{Dif} = R_{Dif}C_{Dif}$ are the respective time constants. With this notation, the two RC parallels (R_{CT}, C_{CT} and R_{Dif}, C_{Dif}) represent the charge transfer (CT) and diffusion (Dif) phenomena inside the battery. In [19] a detailed representation of these battery phenomena is addressed: diffusion and charge transfer properties are described with more impedance elements, with specific dependence on the input current.

The output equation of the model relates the average output voltage $V(k)$ of the cell model to the open circuit voltage V_{OCV} and the voltage drops across the elements, as follows:

$$V(k) = V_{OCV}(SoC(k)) - V_{CT}(k) - V_{Dif}(k) - R_0 I(k) \quad (2)$$

where R_0 is the battery cell internal resistance.

Defining the state vector $x(k) = [SoC(k) \ V_{CT}(k) \ V_{Dif}(k)]^T$, the model input $u(k) = I(k)$ and output $y(k) = V(k)$, the discrete-time non-linear state space battery model is written as:

$$\begin{cases} x(k) = Ax(k) + Bu(k) \\ y(k) = g(x(k), u(k)) \end{cases} \quad (3)$$

The non linearity of the model is in the output equation (2), non linear with reference to the state $x(k)$, while the state equation is linear and the system matrices are defined as:

$$A = \begin{bmatrix} 1 & 0 & 0 \\ 0 & e^{-\frac{\Delta t}{\tau_{CT}}} & 0 \\ 0 & 0 & e^{-\frac{\Delta t}{\tau_{Dif}}} \end{bmatrix} \quad B = \begin{bmatrix} -\frac{\Delta t}{Q_{nom}} \\ R_{CT} \left(1 - e^{-\frac{\Delta t}{\tau_{CT}}}\right) \\ R_{Dif} \left(1 - e^{-\frac{\Delta t}{\tau_{Dif}}}\right) \end{bmatrix} \quad (4)$$

The battery cell model (3) is defined as a function of the dynamic parameters $R_{CT}, C_{CT}, R_{Dif}, C_{Dif}$, of the open circuit voltage V_{OCV} and the resistance R_0 . The identification of these parameters is discussed in Section III.

III. PARAMETERS IDENTIFICATION

The dynamic parameters R_{CT}, C_{CT}, R_{Dif} and C_{Dif} were identified by cell/pack testing and *AllCell Technologies*.

Their values are presented in Table I. A dependence of these parameters from *SoC* is not taken into account as a wide variation of the parameters values with reference to the *SoC* has not registered during testing. In addition, experimental measurements to define the parameters dependency on *SoC* are accurate when *SoC* value is higher than 10%.

TABLE I: Dynamic parameters values

R_{CT}	$1.6\text{m}\Omega$
$\tau_{CT} = R_{CT}C_{CT}$	3.68s
R_{Dif}	$7.7\text{m}\Omega$
$\tau_{Dif} = R_{Dif}C_{Dif}$	84.34s

Several characterization tests were conducted at ambient temperatures. For the purpose of this work the temperature dependence of the model parameters is not taken into account and the ambient temperature is considered the reference operative thermal condition.

From experimental tests, the relationship between the open circuit voltage V_{OCV} and state of charge *SoC* has been also identified. The $V_{OCV}(SoC)$ is shown in Fig. 2.

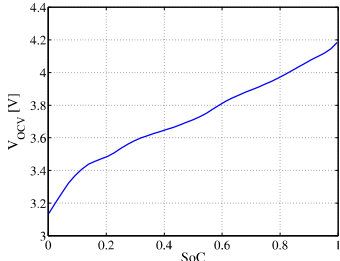


Fig. 2: V_{OCV} characteristic, function of *SoC*

Within this model, the left parameter to identify is the battery cell resistance R_0 . For R_0 identification, a battery discharge test has established, as shown in Fig. 3 where the current profile in Fig. 3(a) is given as input and the voltage response in Fig. 3(b) is registered as output. During the test the battery is completely discharged, starting from a full charged condition. With reference to the e-bike application, the only discharge scenario is evaluated, since regeneration is not possible on board of the vehicle.

In the next Sections III-A an EKF algorithm for the resistance R_0 identification is shown. The results are compared to the case where the resistance is identified through Least Square (LS) in Section III-B.

A. Extended Kalman Filter for Resistance and Capacity estimation

The Extended Kalman Filter is a well known algorithm largely used [20]–[22] to estimate the state of a dynamic system characterized by noisy measurements. At the same time, this method may also be used to perform system parameters identification starting from experimental data [22].

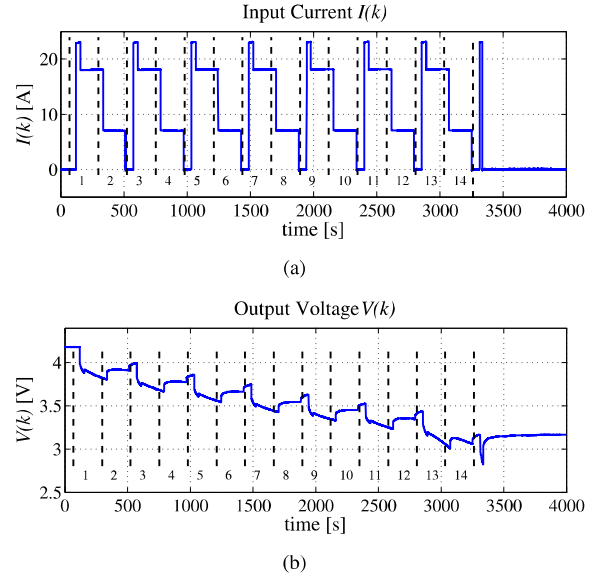


Fig. 3: (a) Experimental Input current; (b) Experimental output voltage

In this paper we use EKF to identify the resistance R_0 of the second order Randle model in Fig. 1. In addition to that, we also use EKF to identify the battery capacity Q_{nom} . The experimental discharging test used for parameter identification (Fig. 3) is performed on a battery at its Beginning of Life (BOL) and the battery cell capacity value at BOL is declared by the constructor. With the EKF this parameter Q_{nom} is estimated in order to verify the accuracy of the cell capacity value.

Following the same structure of [22], the parameters to identify are included in the parameters vector θ , as follows:

$$\theta = [R_0 \quad Q_{nom}]^T \quad (5)$$

Hence, the state space battery model (3) can be written as:

$$\begin{cases} x(k+1, \theta) = Ax(k) + B(\theta)u(k) \\ y(k, \theta) = g(x(k), u(k), \theta) \end{cases} \quad (6)$$

where the dependence of the parameters vector θ is now made explicit.

The EKF is a model based method for the state estimation. To identify the vector of parameters, θ has to be considered as the state of a proper state space model. For this reason a constant dynamic behavior for θ is modeled as:

$$\theta(k+1) = \theta(k) + v_\theta(k) \quad (7)$$

where $v_\theta \sim \mathcal{N}(0, Q_\theta)$ is a white noise gaussian distributed, with zero mean and covariance Q_θ . The model (7) is justified by the fact that the aging parameters R_0 and Q_{nom} vary very slowly compared to the system dynamics (3). The noise v_θ models uncertainties associated with the model (7). Given that the constant dynamic behavior of θ is quite accurate, the covariance of v_θ is set to be quite small.

The output equation is a measurable function of the system

parameters θ :

$$y_\theta(k, \theta) = g(x(k), u(k), \theta(k)) + w_\theta(k) \quad (8)$$

This is the same output equation of the battery model, since the battery voltage experimentally measured, indicated by V_{exp} , is used for the identification. $w_\theta \sim \mathcal{N}(0, R_\theta)$ is a white gaussian noise with zero mean and covariance R_θ which represents the model output noise.

Due to the non linearity of the model here considered, the Extended version of the Kalman filter has to be used. A summary of a nonlinear EKF algorithm equations is shown in Table II, defined by the prediction and correction steps [8].

TABLE II: Extended Kalman filter algorithm for parameters identification

Prediction Step:	$\hat{\theta}^-(k) = \hat{\theta}(k-1)$	(9a)
	$P_\theta^-(k) = P_\theta(k-1) + Q_\theta$	(9b)
Correction Step:		
	$L_\theta(k) = P_\theta^-(k)C_\theta(k)^T (C_\theta(k)P_\theta^-(k)C_\theta(k)^T + R_\theta)^{-1}$	(10a)
	$\hat{\theta}(k) = \hat{\theta}^-(k) + L_\theta(k)[V_{exp}(k) - g(x(k), u(k), \hat{\theta}^-(k))]$	(10b)
	$P_\theta(k) = (I - L_\theta(k)C_\theta(k))P_\theta^-(k)$	(10c)

In the prediction step, the estimated state $\hat{\theta}$ and its covariance matrix P_θ are projected to the next time step using the dynamic model equation defined for θ in (7) and the noise covariance Q_θ respectively. The superscript minus indicates that these quantities in (9a) and (9b) have not yet been corrected using the measurement [8], as done in (10b) and (10c). In the correction step, the parameters vector estimation $\hat{\theta}$ and its covariance P_θ are corrected by using the information from the measurements and the adapted Kalman gain L_θ . In this way, $\hat{\theta}$ is the parameters vector estimation, in order to reduce the difference between the experimental voltage $V_{exp}(k)$ and the model response $g(x(k), u(k), \hat{\theta}^-(k))$. It has to be noticed that to evaluate this last term, the model state $x(k)$ is necessary; this can be evaluated from the model itself, integrating the system equations (1), starting from the initial conditions corresponding to $SoC(0) = 100\%$ and $V_{CT}(0) = V_{Dif}(0) = 0V$, with reference to the experimental test shown in Fig 3.

The matrix C_θ , used in (10a) and (10c), represents the linearization of the non linear output equation (8), with respect to the vector of parameters θ :

$$C_\theta(k) = \left. \frac{dg(x(k), u(k), \theta(k))}{d\theta} \right|_{\theta=\hat{\theta}^-(k)} \quad (11)$$

As also shown in [22], since the non linear function $g(x(k), u(k), \theta(k))$ is function of both the parameters vector $\theta(k)$ and the battery model state $x(k)$, (11) can be written as:

$$\left. \frac{dg(x, u, \theta)}{d\theta} \right|_k = \left. \frac{\partial g(x, u, \theta)}{\partial \theta} \right|_k + \left. \frac{\partial g(x, u, \theta)}{\partial x} \right|_k \left(\left. \frac{dx}{d\theta} \right|_k \right) \quad (12)$$

$$\left. \frac{dx}{d\theta} \right|_k = \left. \frac{\partial B(\theta)}{\partial \theta} \right|_{k-1} u(k-1) + A \left(\left. \frac{dx}{d\theta} \right|_{k-1} \right) \quad (13)$$

The term $\left. \frac{dx}{d\theta} \right|_k$ is initialized at 0 and evolves following the dynamics in (13). In this work, since the vector θ is defined as in (5), through (12) (13) the matrix $C_\theta(k)$ can be computed as:

$$C_\theta(k) = \begin{bmatrix} -I(k) & 0 \\ 0 & \frac{\Delta t I(k-1)}{Q_{nom}^2(k-1)} \\ 0 & 0 \\ 0 & 0 \end{bmatrix} + A \frac{dx(k-1)}{d\theta} \quad (14)$$

where $C = \frac{\partial g(x, I, \theta)}{\partial x}$ and A is the dynamic matrix of the battery model shown in (4).

The values used for the state and output noise covariance in this work are $Q_\theta = \begin{bmatrix} 10^{-6} & 0 \\ 0 & 10^{-4} \end{bmatrix}$ and $R_\theta = 10$. The noise v_θ has a weak effect on the constant dynamics of the parameters, while a larger output covariance is accepted for w_θ , in order to consider generic uncertainties on the overall model.

In Fig. 4 the estimated resistance \hat{R}_0 is shown (dashed line). In Fig. 5 it is shown a comparison between the model response \hat{V}_{mod} when using this value of R_0 , and the experimental data V_{exp} . To quantify how close the model output is to the measurements, the validation error \tilde{e}_{EKF} is evaluated as:

$$\tilde{e}_{EKF}(k) = V_{exp}(k) - \hat{V}_{mod}(k) \quad (15)$$

where V_{exp} is the experimental voltage measurement and \hat{V}_{mod} is the model output voltage, computed using (2) where \hat{R}_0 is used. The error \tilde{e}_{EKF} is shown in Fig. 6 and its RMS value is shown in Table III.

The capacity value \hat{Q}_{nom} estimated with this approach is practically constant over the simulation time window, and equivalent to its nominal value $Q_{nom} = 10.4 Ah$: this confirms that the original value of the nominal capacity can be considered correct for the battery model, and a variation of this value due to aging phenomena is not relevant on a short time window.

With regard to the resistance \hat{R}_0 , in Fig. 4 a dependence of \hat{R}_0 on SoC is noticeable. In order to include and identify the resistance dependence on the SoC , in the next section a Least Squares method is used for the identification of $R_0(SoC)$.

B. Least Squares Methods for Resistance identification

It is known that battery resistance is function of SoC [23]. This is also confirmed by the results of the resistance estimation \hat{R}_0 via EKF in the previous section. In this section, a Least Squares method is considered to better identify this dependence and define $R_0(SoC)$.

To apply the LS method, the input and output collected data are divided into SoC batches, as shown in Fig. 3. For each batch i , a constant resistance value $\hat{R}_{0,i}$ is identified minimizing the sum of the squared difference S_i between the experimental measured voltages $V_{exp,i}$ and the voltage

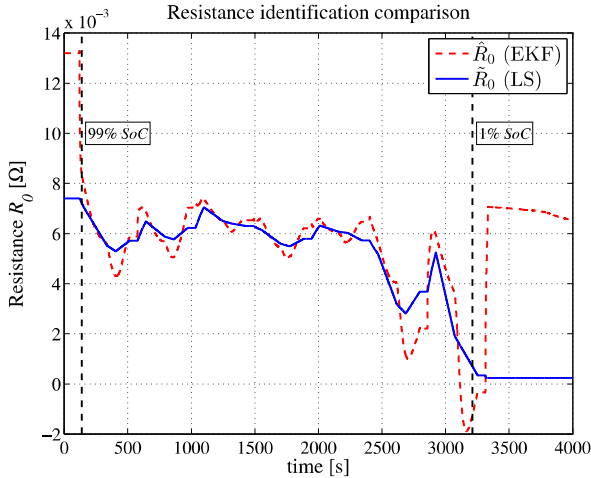


Fig. 4: Comparison between \hat{R}_0 estimated with EKF and \tilde{R}_0 identified with LS approach

predicted by the model output relation (3):

$$\min(S_i) = \min \left(\sum_{j=T_{0,i}}^{T_{f,i}} (V_{exp,i}(j) - g(x(j), u(j), \tilde{R}_{0,i}))^2 \right) \quad (16)$$

$T_{0,i}$ and $T_{f,i}$ are the initial and final time instant of each batch i respectively. As shown in Section II, the output function $g(\cdot)$ has a linear dependence on the parameter $\tilde{R}_{0,i}$ and the input $u(k)$, and it is non linear with reference to the model state $x(k)$. To apply the LS method, the input $u(k)$ and the state $x(k)$ are known at each time instant, the former from experimental measurements and the latter from the model integrating the equation (1); this is possible since the current measurements are accurate and the values $SoC(0) = 100\%$ and $V_{CT}(0) = V_{Dif}(0) = 0V$ are considered as initial conditions.

In Fig. 4 (solid line) the LS-estimated results $\tilde{R}_0(SoC(k))$ is shown as function of time, since the $SoC(k)$ is known integrating the model equation. Comparing \hat{R}_0 evaluated with EKF and \tilde{R}_0 with LS method both as a function of time, from Fig. 4 it can be seen that the two show similar trends over the entire SoC range except for high SoC (beginning of discharging, 99% SoC) and low SoC values (1%).

Also in this case the validation error \tilde{e}_{LS} is evaluated as the difference between experimental voltage $V_{exp}(k)$ and the model output \tilde{V}_{mod} when $\tilde{R}_0(SoC)$ is used:

$$\tilde{e}_{LS}(k) = V_{exp}(k) - \tilde{V}_{mod}(k) \quad (17)$$

The error \tilde{e}_{LS} is shown in Fig. 6. In addition, in Table III the error RMS value of \tilde{e}_{EKF} and \tilde{e}_{LS} are compared, while in Fig. 5 the model output voltages $\hat{V}_{mod}(k)$ and $\tilde{V}_{mod}(k)$ evaluated using \hat{R}_0 and $\tilde{R}_0(SoC)$ are shown respectively.

Even if the RMS value of \tilde{e}_{EKF} in Table III is slightly better, from Fig. 5 and Fig. 6 it is clear that validation performances are comparable between the EKF and LS approach. Thus the resistance identification performed with LS method here presented well describes the the resistance dependence $\tilde{R}_0(SoC)$ on the SoC and it will be used in the

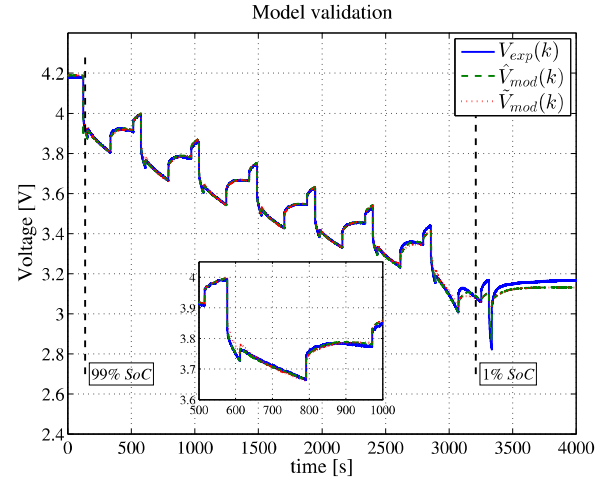


Fig. 5: Comparison between experimental output voltage $V_{exp}(k)$, $\hat{V}_{mod}(k)$ evaluated with \hat{R}_0 (EKF) and $\tilde{V}_{mod}(k)$ using \tilde{R}_0 (LS)

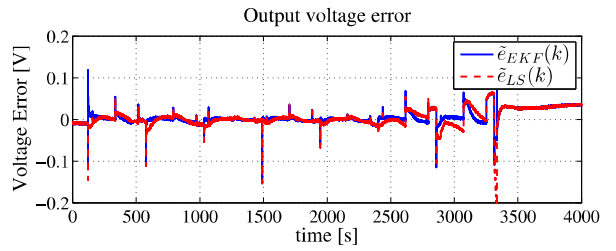


Fig. 6: Comparison between the validation error $\tilde{e}_{EKF}(k)$ and $\tilde{e}_{LS}(k)$

TABLE III: Validation RMS error, comparison between EKF method and LS approach

Error	RMS value
$\tilde{e}_{EKF}(k)$	$0.01694 V^2$
$\tilde{e}_{LS}(k)$	$0.0216 V^2$

state space battery model.

In order to obtain a good SoC estimation with model based algorithms, the accuracy of the state space model is a crucial point to get good performances. In the next section, SoC estimation problem is addressed based on the model here identified.

IV. SoC ESTIMATION ALGORITHMS

In this paper, for the SoC estimation an EKF is designed along with an adaptive version of the Kalman filter where the process covariance matrix is adaptively updated.

A. Extended Kalman Filter

In this work, the SoC estimation problem for an e-bike application is addressed, with the purpose to define an algorithm suitable for on board implementation, in order to improve the battery usage and the vehicle power management.

In this section, the EKF is considered with reference to the model (3) introduced in Section II and identified in Section

III. Here it is proposed with the addition of the gaussian noise on the state and the output equation, as Kalman assumption:

$$\begin{cases} x(k+1) = Ax(k) + Bu(k) + v(k) \\ V(k) = g(x(k), u(k)) + w(k) \end{cases} \quad (18)$$

where $v(k) \sim \mathcal{N}(0, Q)$ and $w(k) \sim \mathcal{N}(0, R)$ are white gaussian noises with zero means and covariance matrices Q for the model state equation and R for the output relation respectively. The estimator equations are summarized in Table IV.

TABLE IV: Summary of Extended Kalman filter algorithm equations

Prediction Step:	
$\hat{x}^-(k) = A\hat{x}(k-1)A^T + Bu(k-1)$	(19a)
$P^-(k) = AP(k-1)A^T + Q$	(19b)
Correction Step:	
$L(k) = P^-(k)C(k)^T (C(k)P^-(k)C(k)^T + R)^{-1}$	(20a)
$\hat{x}(k) = \hat{x}^-(k) + L(k)[V_{exp}(k) - g(\hat{x}^-(k), u(k))]$	(20b)
$P(k) = (I - L(k)C(k))P^-(k)$	(20c)

A brief description of the Kalman prediction and correction step was already given in Section III-A. Matrices $L(k)$ and $P = E[e(k) \cdot e(k)^T]$ are respectively the Kalman gain and the covariance matrix of the estimation error $e(k) = x(k) - \hat{x}(k)$.

Matrix $C = \frac{\partial g(x, I, \theta)}{\partial x}$, used in the filter equations (20a) and (20c), is the linearized output matrix.

With regards to the choice of the noises statistical parameters Q and R , matrix Q is designed under the assumption that there is no correlation between the noise on different state components [11], leading to a diagonal structure. The state noise $v(k)$ represents the model uncertainties as well as the approximation due to the non-linearities not considered, which cause the battery dynamic behaviour not to be completely represented by the model [10]. The designed matrix $Q = \begin{bmatrix} 1000 \cdot R & 0 & 0 \\ 0 & 0.1 \cdot R & 0 \\ 0 & 0 & 0.01 \cdot R \end{bmatrix}$, defined with reference to the matrix R , presents a higher weight on the first component of the state $x(k)$, since the main interest is in the *SoC* estimation.

The output noise covariance R is evaluated using the experimental data and considering the model validation error $\tilde{e}_{LS}(k)$ computed with (17): from a statistical analysis of the error itself, it is can be shown that $\tilde{e}(k)$ is well approximated by a Gaussian distribution with zero mean and the covariance value $R = 8.432 \cdot 10^{-4}$.

In the next section an adaptive version of the EKF is presented.

B. Adaptive Extended Kalman Filter

The idea behind the *adaptive-EKF* is to update the statistical noises covariance parameters Q and R in order to improve the estimation performances. In a Kalman filter, the *a priori* covariance values for the measurement and process noises

are crucial for the stability and the convergence property of the EKF: a complete knowledge of the process statistical properties is assumed [24]. The works mentioned in the following show that an adaptive update of the covariance matrices improves the estimation results as opposed to a fixed choice of the covariances.

These kind of solutions are successfully used in different research fields: in [25] an AEKF is implemented to estimate the position of a mobile robot, considering a matrix Q with a fixed structure, apart from a scaling factor which is adaptively changed. A different adaptive law is shown in [24], where the adaptive filter is used in particular to deal with asynchronous measurement in a tank reactor.

AEKF algorithm has been used also for battery *SoC* estimation. In [26] the process covariance matrix is updated online with a dedicated estimator. In [27] the adaptive algorithm is activated only when the estimation is diverging, in order to keep it stable. In both the cases, particular attention is made on the accuracy of the model, with parameters estimation realized respectively with neural networks and the filter itself. In [28] a solution more similar to the following is proposed, but for a different type of battery (Lead-Acid) and application.

AEKFs have been used also to solve the problem of inertial navigation system/global positioning system (INS/GPS). In these applications a problem of data fusion is addressed, since INS sensors are used: they represent a cheap solution and also not so accurate. For this reason, it is not easy to define good *a priori* statistical parameters values, due mainly to their large variability of the sensor noise: this is directly related to the accuracy of position estimation. The adaptive solution can deal with this problem, providing a choice of the noises covariance parameters Q and R , representing also a solution for system interaction [29]–[31]. In all these works the adaptive algorithm proposed in [32] is validated and the good results of this approach are confirmed.

In this work, the adaptive law for the process covariance Q proposed in [32] for INS/GPS application is used. An adaptive update of matrix Q can help in overcoming the uncertainties in the noise properties, which represent model uncertainties due to the identification process and non-linearities not included.

An adaptive choice for matrix R is not investigated, since a reliable analysis of the measurement covariance R is possible starting from the model validation, as shown in Section IV-A.

In all the adaptive algorithms here mentioned, the estimation performance is considered through the information represented by the innovation sequence $d(k)$. The innovation $d(k)$ is defined:

$$d(k) = V_{exp}(k) - g(\hat{x}^-(k), u(k)) \quad (21)$$

It is the difference between the experimental voltage measurement $V_{exp}(k)$ and the predicted value $g(\hat{x}^-(k), u(k))$. In $d(k)$ the predicted voltage is computed by the model output equation when the state in the prediction step $\hat{x}^-(k)$ is taken into account.

The innovation covariance matrix is computed as:

$$\hat{D}(k) = \frac{1}{N} \sum_{i=i_0}^N d(i)d(i)^T \quad (22)$$

using a moving average of $d(k)$ evaluated in (21), inside a moving estimation window of size N , where $j_0 = k - N + 1$ is the first instant inside the window.

Matrix $\hat{D}(k)$ represents the actual performance of the estimation process, so that it is a crucial element to be used in defining the adaptive law for matrix Q . The choice of the window length N become a design parameter for the algorithm: it must be not so small to correctly represent the estimation performance and at the same time, for on-board implementation, it has to consider the memory available on a physical board.

Starting from the evaluation of $\hat{D}(k)$, the *innovation based adaptive Kalman filter* can be used, as demonstrated in [32]. The innovative contribution in [32] is the formulation of the filter in terms of maximum likelihood (ML) estimator. The advantage of this approach is to define some adaptive parameters to be used in the traditional EKF estimator. A ML equation is defined, function of these adaptive parameters. In this work, the only adaptive parameter considered is the process noise covariance matrix Q . The ML equation represents the mathematical condition which allows to derive an adaptive law for the matrix Q function of the innovation covariance matrix $\hat{D}(k)$. Under the assumption that the measurement noise covariance R is taken as constant, the ML equation in [32] can be transformed in:

$$\hat{Q}(k) = \frac{1}{N} \sum_{i=i_0}^N \Delta\hat{x}(i) \Delta\hat{x}(i)^T + P(k) - A P(k-1) A^T \quad (23)$$

where $\Delta\hat{x}$ is the state correction:

$$\Delta x(k) = \hat{x}(k) - \hat{x}^-(k) \quad (24)$$

This is evaluated as the difference between the state before and after updates. From (20b) it can be written:

$$\Delta\hat{x}(k) = L(k) d(k) \quad (25)$$

Substituting (25), (23) can be approximated as [32]:

$$\hat{Q}(k) = L(k) \hat{D}(k) L(k)^T \quad (26)$$

To conclude, the AEKF algorithm for the *SoC* estimation uses the same equation of the EKF filter summarized in Table IV, where the equation (19b) is updated with the adaptive law (26) introduced:

$$P^-(k+1) = A P(k) A^T + \hat{Q}(k)$$

C. Results comparison

EKF and AEKF algorithms are both tested considering the experimental discharge test in Fig. 3. In Fig. 7 it is shown a comparison between $\hat{S}oC_{EKF}$ and $\hat{S}oC_{AEKF}$, the estimated state of charge from the EKF and AEKF algorithms respectively. As a reference for the comparison, state of charge obtained with Coulomb Counting method (SoC_{cc})

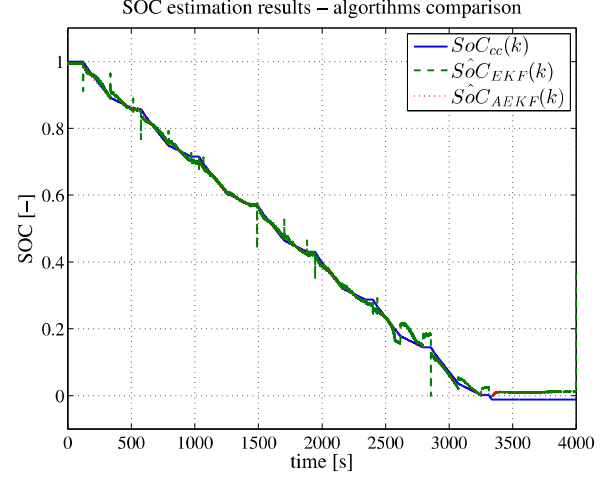


Fig. 7: Comparison between SoC estimation results: reference Coulomb counting SoC_{cc} , \hat{SoC}_{EKF} evaluated with EKF and \hat{SoC}_{AEKF} with AEKF

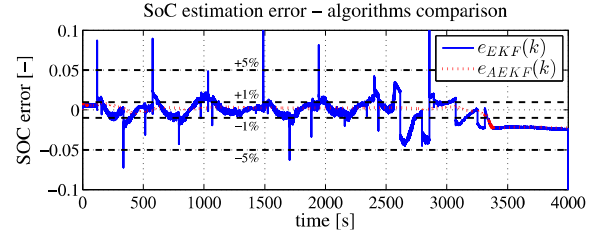


Fig. 8: Comparison between SoC estimation error with EKF algorithm $e_{EKF} = SoC_{cc} - \hat{SoC}_{EKF}$, and error with AEKF $e_{AEKF} = SoC_{cc} - \hat{SoC}_{AEKF}$

considered. SoC_{cc} time discrete domain expression is the *SoC* dynamic equation in the battery model:

$$SoC_{cc}(k+1) = SoC_{cc}(k) - \frac{\Delta t}{Q_{nom}} I(k) \quad (27)$$

In both the cases, the model state is estimated starting from the initialization state $x(0) = [0.4 \ 0 \ 0]^T$, corresponding to an initial $SoC(0) = 0.4$, while the actual level is close to 1, to test the convergence performances of the filters.

As shown in Fig. 8, using EKF the *SoC* estimation error, computed as $e_{EKF}(k) = SoC_{cc}(k) - \hat{SoC}_{EKF}(k)$, remains between the 5% with respect to the SoC_{cc} (Fig 8). This result is related to the performance of the model in reproducing the battery behavior: the choice made in the identification phase, to define a dependence on the *SoC* only for the resistance $R_0(SoC)$, reflects into a non perfect representation of the dynamics of the battery. In addition, where the model error is greater (Fig. 6), and in particular for very low *SoC* values, also the estimation becomes more difficult.

With the AEKF a substantial improvement in the estimation performance is achieved, as shown in Fig. 7. Form Fig. 8 the estimation error $e_{AEKF}(k) = SoC_{cc}(k) - \hat{SoC}_{AEKF}(k)$ in this case remains close to 1%, a good improvement with reference to the EKF, thanks to the adaptive update of the covariance Q . In this way, the uncertainty of the model are adaptively compensated since $\hat{Q}(k)$ changes following the estimation error. Also for low values of *SoC* the overall

performance are better, even if is not possible to assure a perfect estimation very close to zero value of SoC .

About the convergence, both filters show a quick response. In AEKF in particular, the convergence time depends on the first choice of $\hat{Q}(0)$ in the initialization phase: the values $\hat{Q}(0) = Q$, corresponding to the constant Q used for the EKF, is chosen. It has been verified that even starting with a poor initialization, the AEKF estimation performances are however good after a first convergence period.

V. CONCLUSIONS

In this work, a state space model for a Li-ion battery design by AllCell Technologies for light vehicle application, such as e-bikes, has been defined. Model parameters have been experimentally identified. A comparison between EKF and LS identification methods, to identify the resistance dependence on SoC , has been performed. In this way a good model validation is achieved.

An EKF for SoC estimation and an adaptive improvement of the estimator have been presented. These algorithms have been implemented in simulation and the estimation results are compared. The choice of an adaptive law for the process noise covariance matrix shows an improvement in estimation performances. In terms of estimation error, the EKF results are into 5% estimation error range, while with AEKF this range is reduced up to 1%.

ACKNOWLEDGEMENT

This work is supported by AllCell Technology. The collaboration with Peter Sveum, Sebastien Maes and Naz Al-Khayat is gratefully acknowledged.

REFERENCES

- [1] Wen-Yeau Chang. The state of charge estimating methods for battery: a review. *ISRN Applied Mathematics*, 2013.
- [2] Shuo Pang, J. Farrell, Jie Du, and M. Barth. Battery state-of-charge estimation. 2:1644–1649 vol.2, 2001.
- [3] John Chiasson and Baskar Vairamohan. Estimating the state of charge of a battery. *IEEE Transactions on Control Systems Technology*, 13(3):465–470, 2005.
- [4] M. Coleman, Chi Kwan Lee, Chunbo Zhu, and W.G. Hurley. State-of-charge determination from emf voltage estimation: Using impedance, terminal voltage, and current for lead-acid and lithium-ion batteries. *Industrial Electronics, IEEE Transactions on*, 54(5):2550–2557, Oct 2007.
- [5] Osvaldo Barbarisi, Francesco Vasca, and Luigi Glielmo. State of charge Kalman filter estimator for automotive batteries. *Control Engineering Practice*, 14(3):267 – 275, 2006. Advances in Automotive Control (AC'04).
- [6] D. Di Domenico, G. Fiengo, and A. Stefanopoulou. Lithium-ion battery state of charge estimation with a Kalman Filter based on a electrochemical model. In *Control Applications, 2008. CCA 2008. IEEE International Conference on*, pages 702–707, Sept 2008.
- [7] Sabine Piller, Marion Perrin, and Andreas Jossen. Methods for state-of-charge determination and their applications. *Journal of Power Sources*, 96(1):113 – 120, 2001. Proceedings of the 22nd International Power Sources Symposium.
- [8] M. Rubagotti, S. Onori, and G. Rizzoni. Automotive Battery Prognostics Using Dual Extended Kalman Filter. pages 257–263, Oct 2009.
- [9] Gregory L. Plett. Extended Kalman filtering for battery management systems of LiPB-based HEV battery packs: Part 3. State and parameter estimation. *Journal of Power Sources*, 134(2):277 – 292, 2004.
- [10] Seongjun Lee, Jonghoon Kim, Jaemoon Lee, and B.H. Cho. State-of-charge and capacity estimation of lithium-ion battery using a new open-circuit voltage versus state-of-charge. *Journal of Power Sources*, 185(2):1367 – 1373, 2008.
- [11] Amir Vasebi, Maral Partovibakhsh, and S. Mohammad Taghi Bathaei. A novel combined battery model for state-of-charge estimation in lead-acid batteries based on extended kalman filter for hybrid electric vehicle applications. *Journal of Power Sources*, 174(1):30 – 40, 2007. Hybrid Electric Vehicles.
- [12] Parthasarathy M. Gomadam, John W. Weidner, Roger A. Dougal, and Ralph E. White. Mathematical modeling of lithium-ion and nickel battery systems. *Journal of Power Sources*, 110(2):267 – 284, 2002.
- [13] O. Tremblay, L-A Dessaint, and A-I. Dekkiche. A Generic Battery Model for the Dynamic Simulation of Hybrid Electric Vehicles. pages 284–289, Sept 2007.
- [14] F. Codeca, S.M. Savaresi, and G. Rizzoni. On battery State of Charge estimation: A new mixed algorithm. pages 102–107, Sept 2008.
- [15] Lijun Gao, Shengyi Liu, and R.A. Dougal. Dynamic lithium-ion battery model for system simulation. *Components and Packaging Technologies, IEEE Transactions on*, 25(3):495–505, Sep 2002.
- [16] Githin K. Prasad and Christopher D. Rahn. Development of a first principles equivalent circuit model for a lithium ion battery. In *ASME 2012 5th Annual Dynamic Systems and Control Conference joint with the JSME 2012 11th Motion and Vibration Conference*, pages 369–375. American Society of Mechanical Engineers, 2012.
- [17] M. Ceraolo. New dynamical models of lead-acid batteries. *Power Systems, IEEE Transactions on*, 15(4):1184–1190, Nov 2000.
- [18] S.S. Zhang, K. Xu, and T.R. Jow. Electrochemical impedance study on the low temperature of Li-ion batteries. *Electrochimica Acta*, 49(7):1057 – 1061, 2004.
- [19] P.L. Moss, G. Au, E.J. Plichta, and J.P. Zheng. An electrical circuit for modeling the dynamic response of li-ion polymer batteries. *Journal of The Electrochemical Society*, 155(12):A986–A994, 2008.
- [20] Greg Welch and Gary Bishop. An introduction to the Kalman Filter. 1995.
- [21] Gregory L. Plett. Extended Kalman filtering for battery management systems of LiPB-based HEV battery packs: Part 1. Background. *Journal of Power Sources*, 134(2):252 – 261, 2004.
- [22] Gregory L. Plett. Extended Kalman filtering for battery management systems of LiPB-based HEV battery packs: Part 2. Modeling and identification. *Journal of Power Sources*, 134(2):262 – 276, 2004.
- [23] Xuezhe Wei, Bing Zhu, and Wei Xu. Internal resistance identification in vehicle power lithium-ion battery and application in lifetime evaluation. 3:388–392, April 2009.
- [24] Vahid Fathabadi, Mehdi Shahbazian, Karim Salahshour, and Lotfollah Jargani. Comparison of adaptive Kalman filter methods in state estimation of a nonlinear system using asynchronous measurements. 2, 2009.
- [25] L. Jetto, S. Longhi, and G. Venturini. Development and experimental validation of an adaptive extended Kalman filter for the localization of mobile robots. *Robotics and Automation, IEEE Transactions on*, 15(2):219–229, Apr 1999.
- [26] M. Charkhgard and M. Farrokhi. State-of-Charge Estimation for Lithium-Ion Batteries Using Neural Networks and EKF. *Industrial Electronics, IEEE Transactions on*, 57(12):4178–4187, Dec 2010.
- [27] Hongwen He, Rui Xiong, Xiaowei Zhang, Fengchun Sun, and JinXin Fan. State-of-Charge Estimation of the Lithium-Ion Battery Using an Adaptive Extended Kalman Filter Based on an Improved Thevenin Model. *Vehicular Technology, IEEE Transactions on*, 60(4):1461–1469, May 2011.
- [28] Jaeyyun Han, Dongchul Kim, and Myoungho Sunwoo. State-of-charge estimation of lead-acid batteries using an adaptive extended Kalman filter. *Journal of Power Sources*, 188(2):606 – 612, 2009.
- [29] Christopher Hide, Terry Moore, and Martin Smith. Adaptive Kalman filtering for low-cost INS/GPS. *The Journal of Navigation*, 56(01):143–152, 2003.
- [30] C. Hide, T. Moore, and M. Smith. Adaptive Kalman filtering algorithms for integrating GPS and low cost INS. In *Position Location and Navigation Symposium, 2004. PLANS 2004*, pages 227–233, April 2004.
- [31] W. Ding, D.J. Wang, and C. Rizos. Stochastic modelling strategies in GPS/INS data fusion process. 2006.
- [32] A.H. Mohamed and K.P. Schwarz. Adaptive Kalman filtering for INS/GPS. *Journal of geodesy*, 73(4):193–203, 1999.